THE JOURNAL OF PHYSICAL CHEMISTRY C

ARTICLE

pubs.acs.org/JPCC

Study on Polymer Binders for High-Capacity SiO Negative Electrode of Li-Ion Batteries

Shinichi Komaba,*,† Keiji Shimomura,† Naoaki Yabuuchi,† Tomoaki Ozeki,† Hiroharu Yui,‡ and Kohzo Konno‡

†Department of Applied Chemistry, ‡Department of Chemistry, Tokyo University of Science, 1-3 Kagurazaka, Shinjuku, Tokyo 162-8601, Japan

Supporting Information

ABSTRACT: High-capacity SiO powder composite electrodes for rechargeable lithium-ion batteries are prepared with different polymer binders of poly(acrylic acid) (PAA), poly(vinyl alcohol) (PVA), sodium carboxymethyl cellulose (CMCNa), and conventional poly(vinylidene fluoride) (PVdF). Electrode performance of the SiO composites highly depends on selection of binders, and their electrochemical reversibility is drastically improved by using PAA as the binder in comparison to the PVdF, CMCNa, and PVA binders. Coulombic efficiency at the initial cycle is improved for the SiO−PAA composite electrode, and the reversible capacity reaches 700−750 mAh g^{-1} for continuous fifty cycling test at a rate of 100 mA g^{-1}. The improvement mechanism of SiO−PAA composite electrode is characterized by X-ray diffraction, electron microscopy, X-ray photoelectron spectroscopy, infrared spectroscopy, self-discharge test, and adhesive strength test. Amorphous PAA polymer not only tightly binds but also covers the individual SiO particles. Moreover, the PAA binder suppresses swelling of the composite electrode with the electrolyte solution compared to the PVdF binder. Through-thickness electric resistance of the PAA composite electrode is much lower than that of the PVdF when it is wet with the electrolyte. It is proposed that these characters of the PAA binder effectively suppress isolation of the SiO powders in the composite electrode associated with the large volume expansion/shrinkage during the lithiation/delithiation processes.

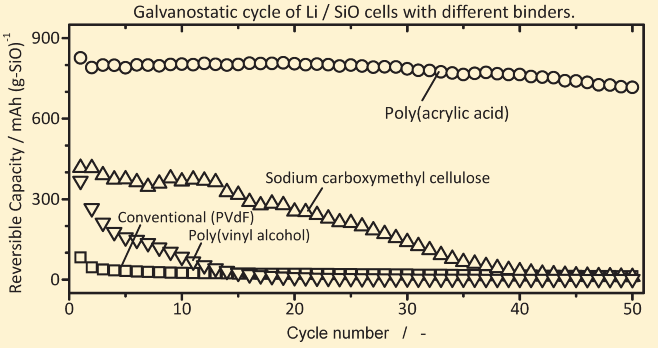

INTRODUCTION

The demand for high-energy lithium-ion batteries is ever increasing. Graphite is the most widely used negative electrode material for the rechargeable lithium-ion batteries because of the necessary advantages, that is, abundant natural resources, very low operating potential close to Li metal, and excellent electrical conductivity. The available capacity of the graphite electrode in a commercial lithium-ion battery reaches more than 350 mAh g^{-1}, which is quite close to the theoretical capacity limit of 372 mAh g^{-1} based on the formation of first stage intercalation compound, that is, LiC_6. Recently, to further enhance the energy density of lithium-ion batteries, silicon-based materials are being widely studied as the negative electrode materials because of high theoretical capacity of electrochemical lithiation. Silicon can electrochemically and reversibly form alloy with lithium at room temperature.[1−7] One mole of silicon can uptake thermodynamically 3.6 mols of lithium, forming $Li_{3.6}Si$. The theoretical capacity of elemental silicon as an electrode is calculated to be 3500 or 1820 mAh g^{-1} based on the weight of Si or $Li_{3.6}Si$, respectively.

However, it is difficult to realize the highly reversible charge and discharge cycle, because large volume expansion (approximately three times larger than the initial volume) upon electrochemical lithiation induces the stress in the particles, thereby resulting in the cracks/fractures of the particles and the following decomposition of an electrolyte solution. This inevitably leads to the isolation of the particles in the composite electrode, exfoliation of the composite electrode from the current collector, and even the collapse of the composite. Recently, electrochemical reactivity of silicon oxide, SiO, consisting of Si and SiO_2 nanodomains, has been reported, which allows for better cycling ability than silicon because of less volume change upon electrochemical cycling.[8−10] It was also proposed that the strain, which originates from the volume expansion, is relieved by lithium silicate domains formed during the electroreduction process. Although the volume expansion of SiO upon electrochemical lithiation is certainly suppressed in comparison to silicon, the reported expansion percentage is still close to 200% of the initial volume, which is significantly larger than that of graphite negative electrode (1.1 times as large as the initial) based on the lithium intercalation reaction into the layered structure.[7,11] Thus, deterioration of the electrochemical

Received: February 21, 2011
Revised: April 14, 2011
Published: June 17, 2011

reversibility of SiO caused by the electronic isolation of the active materials in the composite electrode and exfoliation of the electrode from a current collector, cannot be prevented immediately, especially on the powder based composite electrode.

Recent studies on a binder shed light on the improvement of the reversibility of the composite electrodes using lithium alloying reaction. It was reported that carboxymethyl cellulose (CMC) based binder effectively improves the cycling stability of silicon electrode.[12−17] According to a previous report by Hochgatterer et al., the formation of a covalent chemical bond between the CMC and silicon particle plays an important role in the effective binding and improved performance. Our group reported polyacrylate binders for the graphite negative electrodes, organic radical polymer electrodes, and silicon composite electrodes.[18−21] Recently, poly(acrylic acid) is also investigated as efficient binder for silicon negative electrode by Magasinski et al.[22] We found that the polyacrylate binder uniformly covers graphite particles, and the polyacrylate layer on graphite was found to act as artificial solid electrolyte interphase (SEI) layer.[19,20] Thus, we expect that polyacrylate binder should be much effective binder to improve the cycleability of the SiO composite electrode than the CMC-based binder because of the artificial SEI properties of polyacrylate. In this paper, we examine SiO composite electrode prepared by using polyacrylate binder and compare the results with the conventional poly(vinylidene fluoride) (PVdF), poly(vinyl alcohol) (PVA), and CMC-Na polymeric binders. From these results, we discuss the factors affecting the reversibility and cycleability of high-capacity SiO composite electrode, especially focused on the binding properties of the polymers.

EXPERIMENTAL SECTION

Reagent grade silicon monoxide powder (Aldrich Co. Ltd., ~ 325 mesh), poly(acrylic acid) (PAA, molecular weight (M_v) = 750 000, Sigma-Aldrich Co. Ltd.), sodium carboxymethyl cellulose (CMCNa) (substitution degree = 0.8−1.0, Daicel Chemical Industries, Ltd.), PVA (molecular weight is ca. 110 000, hydrolyzation degree is 97.5−98.5%, Denki Kagaku Kougyou Co. Ltd., Japan), and PVdF (PolySciences, Inc.) were used without any further treatment. PAA, CMCNa, PVA, and PVdF were used as the binder, and their molecular structures are shown in Figure 1.

For the preparation of working electrodes, SiO powder was ball-milled in ambient atmosphere for 24 h at 600 rpm by using a planetary ball-mill (Pulverisette 7, Fritsch Japan Co. Ltd.), thus obtained SiO powders (80 wt %) and acetylene black (10 wt %) were thoroughly mixed with each binder (10 wt %). An adequate amount of *N*-methylpyrrolidinone or distilled water was added for the PVdF or for the PVA, CMCNa, and PAA mixture, respectively. The black slurry thus obtained was cast onto a sheet of copper foil, and predried at 80 °C in air for overnight to remove the solvent. The electrodes were obtained after final dry at 150 °C under a vacuum for 24 h prior to use. The loading of electrodes ranges from 0.89 to 1.7 mg cm^{-2}. Two-electrode 2032-type coin cells (20 mm diameter and 3.2 mm thickness) with the SiO and lithium metal as working and counter electrodes were assembled in an Ar-filled glovebox. An electrolyte solution used was 1 mol dm^{-3} $LiPF_6$ ethylene carbonate (EC)/dimethyl carbonate (DMC) (1:1 by volume). Galvanostatic cycling tests of the SiO electrodes were conducted at a rate of −100 and +100 mA g^{-1} in the voltage range of 0.0−2.0 V at room temperature (ca. 25 °C).

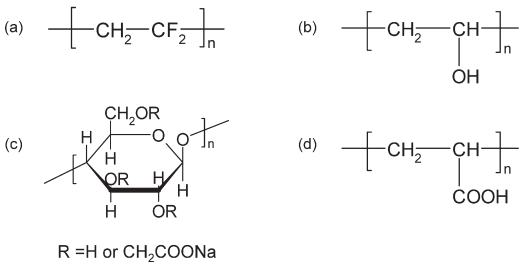

Figure 1. Structures of polymers used as binder for SiO powder electrodes, (a) PVdF, (b) PVA, (c) CMCNa, and (d) PAA.

The SiO electrodes were characterized by scanning electron microscopy (SEM, Hitachi, S-5000, Hitachi High-Technologies Co. Ltd.), X-ray photoelectron spectroscopy (XPS, JPS-9010MC, JEOL Ltd.), X-ray diffraction (XRD, Multi Flex, Rigaku Co. Ltd.), attenuated total reflection-Fourier transform infrared spectroscopy (ATR-FTIR, NICOLET6700, Thermo Scientific. Co. Ltd.), and thermal gravimetric analysis (TGA, DTG-60/60H, Shimadzu Co. Ltd.). Adhesion strength of the SiO composite layer onto the copper foil as current collector was tested using a 180° peel tester (TENSILON, A&D Co. Ltd.). Swelling property of the binders was examined from weight gain of polymer films containing no SiO and acetylene black formed by casting on the Cu foil after soaking in the electrolyte for 24 h. Through-thickness resistance of the SiO composite electrodes on Cu foil was examined by ac impedance method (HP NF ELECTRONIC INSTRUMENTS). The disk-type composite electrode (16 mm in diameter) was tightly sandwiched between two stainless steel plates. The sinusoidal current was applied between the stainless steel plates in the frequency range of 10 kHz−0.1 mHz at the amplitude of 100 μA (root-mean-square value).

RESULTS AND DISCUSSION

Dependence of SiO Electrode Performance on Binders. Galvanostatic reduction and oxidation curves of the SiO electrodes prepared with different four binders are shown in Figure 2 in which the potential variations at the first and second cycles were plotted. A voltage plateau at approximately 0.25 V upon first reduction process of the SiO appears with anomalous irreversible capacity, which could be due to the side reactions, that is, irreversible formation of Li oxide and Li silicates.[23] Figure 2 reveals that the first reduction capacity of the SiO composite electrodes is significantly influenced by selection of the binders. The reduction capacity reaches ca. 1800 mAh g^{-1} for the SiO−PAA electrode, whereas the SiO−PVdF electrode shows less capacity than 300 mAh g^{-1}.

Although the large irreversible capacity can be noticed, the binders of PAA, PVA, and CMCNa allow more than 1000 mAh g^{-1} of the initial reduction capacity as shown in Figure 2. The reversible oxidation capacity of the SiO−PAA electrode reaches 826 mAh g^{-1} at a rate of 100 mA g^{-1} with 38% Coulombic efficiency. In the following cycles after the first one, the SiO−PAA composite electrode can be successfully cycled as is seen in Figure 3. The change in rechargeable capacity of the SiO electrodes prepared with different four binders is compared in Figure 4. The SiO−PVdF electrode shows less than 50 mAh g^{-1} of reversible capacity in this experimental condition,

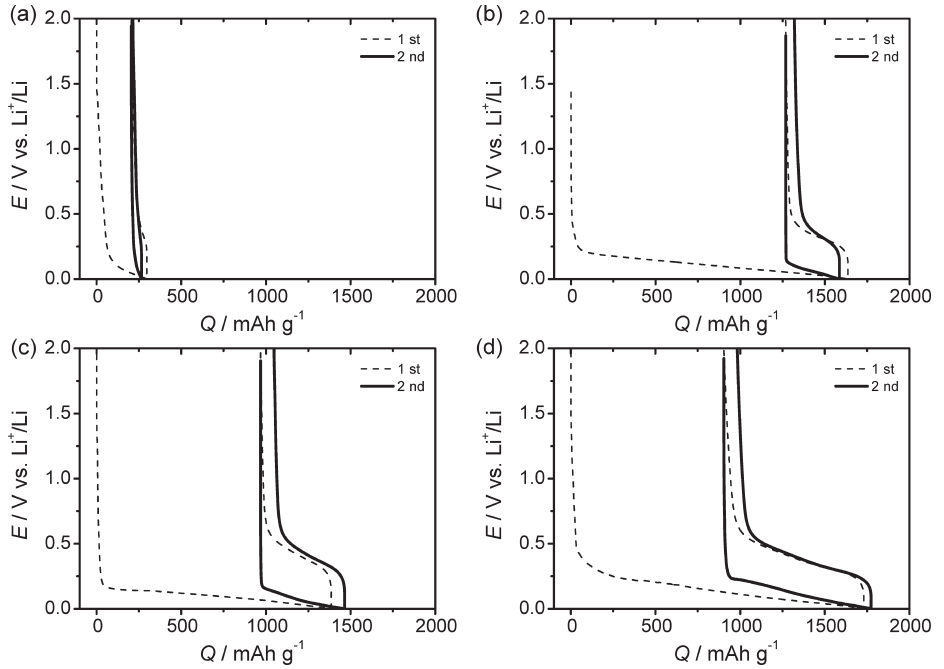

Figure 2. Chronopotentiograms of the SiO powder electrodes prepared with (a) PVdF, (b) PVA, (c) CMCNa, and (d) PAA binders in 1 mol dm-3 LiPF6 EC/DMC solution at a rate of 100 mA g^{-1}.

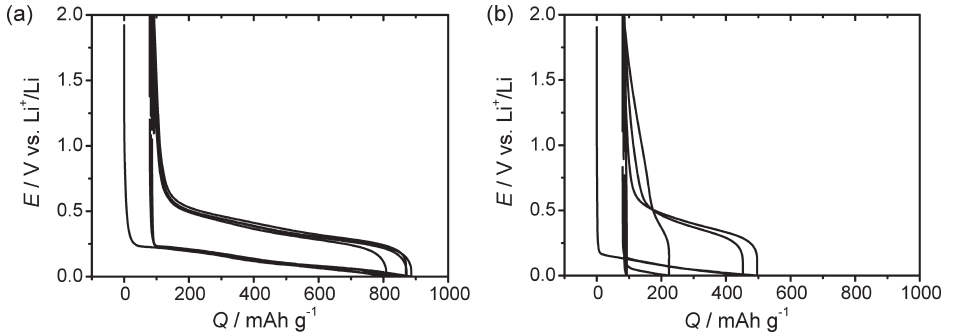

Figure 3. Galvanostatic charge/discharge curves of the SiO composite electrodes prepared with (a) PAA and (b) CMCNa. Sellected charge/discharge cycles at 2nd, 10th, 30th, and 50th cycles are superimposed.

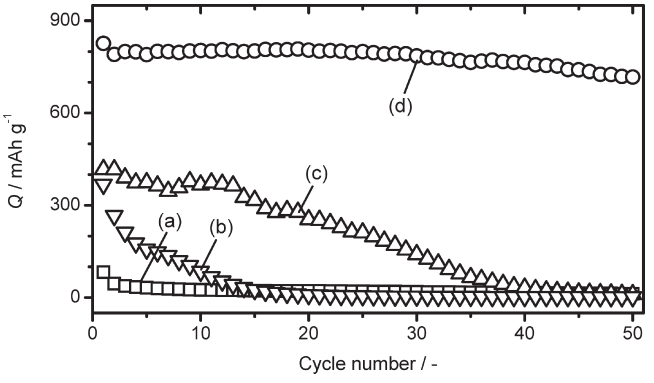

Figure 4. Relation between reversible capacity and cycle number for the SiO composite electrodes prepared with (a) PVdF, (b) PVA, (c) CMCNa, and (d) PAA as a binder.

and the electroactivity was completely depressed by the following several cycles. The SiO−CMCNa and SiO−PVA composite electrodes exhibit similar delithiation capacities of ca. 410 and 370 mAh g^{-1}, respectively, at the initial cycles. Although the CMCNa binder retains higher discharge capacity compared with the PVdF and PVA binders, the reversible capacity of 400 mAh g^{-1} certainly faded during 40 continuous lithiation/delithiation cycles (Figures 3b and 4). In contrast to these binders, the PAA binder clearly improves reversibility of a SiO composite electrode, that is, the reversible capacity of about 700 mAh g^{-1} was retained even over fifty cycles as represented in Figure 4. From these results, it has been concluded that the reversibility of the SiO composite electrodes highly depends on the selection of the binders.

Characterization of SiO Composite Electrodes. To examine the difference in the reversible capacity and cycleability, the surface of SiO−PVdF and SiO−PAA composite electrodes was observed by SEM before and after ten-cycle tests. As shown in Figure 5, the SEM observation confirmed apparent difference in the electrode morphology for the PVdF and PAA electrodes after cycle test. The as-prepared composite electrodes consisted of

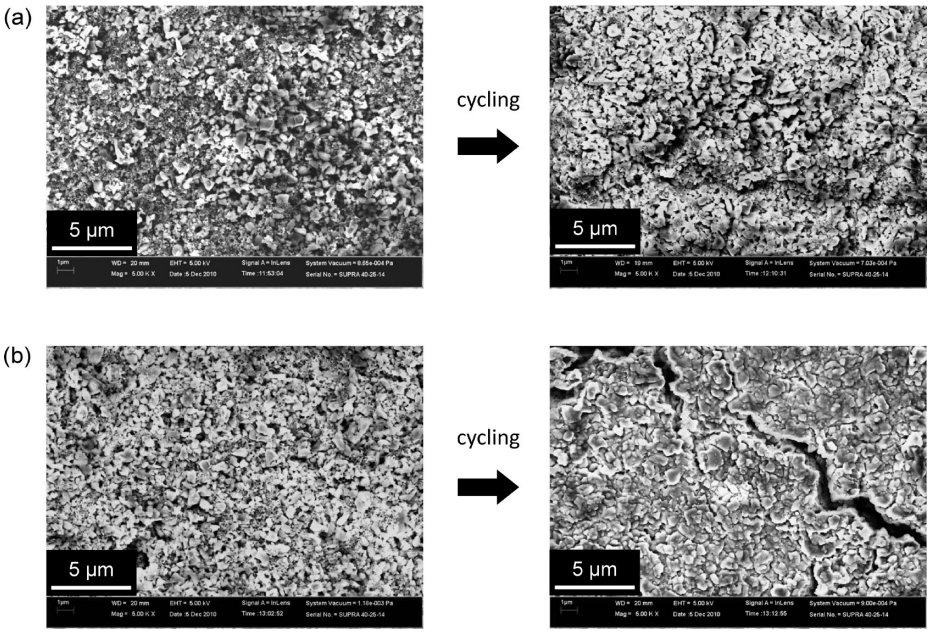

Figure 5. SEM images of the SiO composite electrodes before (left) and after (right) ten charge/discharge cycles prepared with PVdF (a) and PAA (b) binders.

submicrometer-sized SiO particles with dispersed acetylene black, and both electrodes have similar porosity. Before the cycling test, the surface morphology of the SiO composite layer appears to be smooth and flat for both electrodes. The SiO−PVdF electrode showed the much smaller initial charging capacity (~300 mAh g^{-1}) and less reversible capacities than 50 mAh g^{-1} during following cycles, nevertheless, some extent of the deposits was observed on the top of the SiO electrode, and the individual SiO particle appears to be more isolated compared to the as-prepared electrode.

For the SiO−PAA in Figure 5b, the clear changes in the surface morphology of the electrode after cycle are noted: (1) the electrode lost the pores and changed to the dense morphology, and (2) some of the cracks are observed for the cycled electrode. Although the reversibility of the SiO electrode is significantly improved by using the PAA binder, the large reduction capacity (~1800 mAh g^{-1}) during the initial cycle (Figure 2d) inevitably results in the irreversible phase transition, such as formation of lithium silicate, accompanied by the volume expansion. Additionally, irreversible side reactions such as the electrolyte decomposition and formation of the insoluble organic components into the electrolyte would lead to the accumulation of their products in the electrode. The reversible cycling with the higher capacity of ~800 mAh g^{-1} is also accompanied by some extent of the volume change, by which the cracking of the electrodes is induced as observed in the cycled electrode after delithiation. Though there are many cracks on the composite electrode, it is interesting to note that each SiO particle should be still tightly bound within each piece of the cracked parts even after 10 cycling test. Since the SiO particles are not isolated from the current collector, the cracking is not serious electrode damage. This result agrees well with our observation for the graphite-silicon-polyacrylate composite electrode in which the polyacrylate binder protects against the accumulation of the decomposition products of the electrolyte solution and acts as artificial SEI at the surface of graphite and silicon particles as already described.[19−21,24]

Table 1. Adhesion Strength of the SiO Composite Electrodes to the Cu Current Collector Measured by the Peel Test

binder	Average load to peel/N cm^{-1}
PVdF	0.3
PVA	0.7
CMCNa	0.2
PAA	2.3

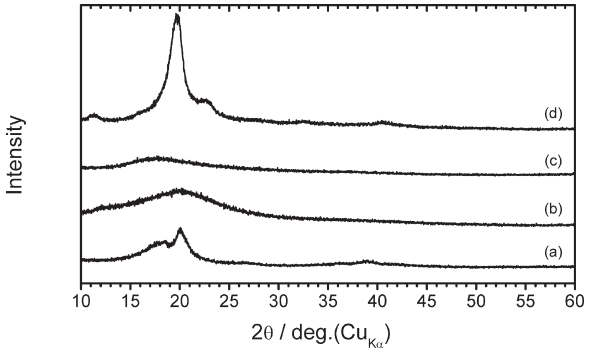

Figure 6. XRD patterns of polymer films: (a) PVdF, (b) CMCNa, (c) PAA, and (d) PVA dried at 150 °C for 24 h.

Adhesion strength of the SiO composite electrodes to the Cu current collector was measured by the peel test. The PVdF, PVA, CMCNa, and PAA composite electrodes were examined and the results are summarized in Table 1. Among the binders examined, the PAA shows the highest adhesion strength to the Cu current collector. The observed value of 2.3 N cm^{-1} for the PAA composite is approximately one order larger than that of PVdF (0.3 N cm^{-1}). The adhesion strength of the composite electrodes corresponds well to the capacity retention as shown in Figures 3 and 4. This implies that the mechanical property of

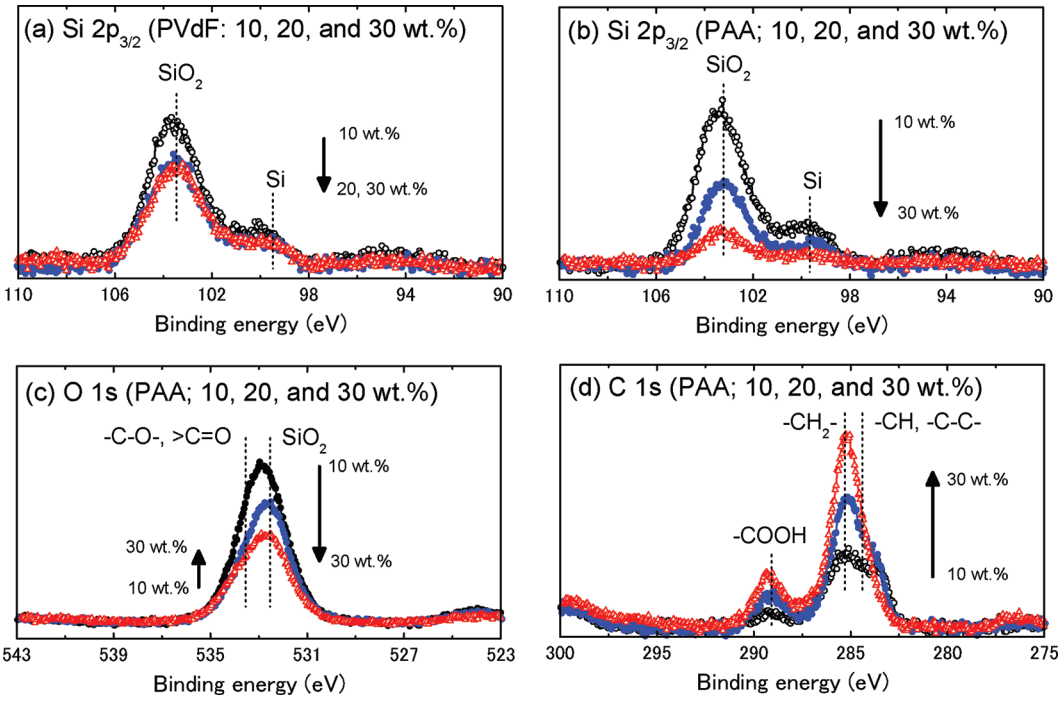

Figure 7. XPS spectra of the composite electrode prepared with different amount of the polymer binders: 10 (open circles), 20 (filled circles), and 30 wt % (open triangles). (a) PVdF composites for Si $2p_{3/2}$ and PAA composite for (b) Si $2p_{3/2}$, (c) O 1s, and (d) C 1s are plotted.

the composite electrode is one of the predominant factors to improve the cycle performance of lithium alloying electrode.

The origin of improved mechanical stability of the composite electrode (Figure 5) and adhesion strength of the composite layer to the Cu current collector (Table 1) would be explained by the difference in the physical and chemical properties of the polymers used as the binder. The crystallinity of the binders used in this study was examined by XRD. Figure 6 shows X-ray diffraction patterns of the polymer films directly formed by the drying of polymer solutions cast onto a zero background sample holder. Since the diffraction peaks are clearly observed around 2θ = ca. 20° for PVdF and PVA polymers, a larger fraction of the polymers is consisting of the crystalline region, whereas CMCNa and PAA polymers become amorphous after casting and drying because of no apparent diffraction lines. The difference in the crystallinity affecting the biding effect will be further discussed in the later section.

Recently, we reported that PAA polymer binder suppressed the cointercalation and decomposition of PC-solvated Li^+ ions and organic cations consisting of room temperature ionic liquid for the graphite negative electrode.[19,24] XPS study suggested that the polyacrylate used as binder uniformly covered the graphite particles, which is different from PVdF, so that the interface between graphite and electrolyte was functionally modified by uniform polyacrylate layer acting as artificial solid-electrolyte interphase (SEI).[19,20] To study the difference in the uniformity of the binders for SiO electrodes, which are covering and/or binding the material particles, surface of the SiO−PVdF and SiO−PAA composites was examined by XPS.

XPS spectra of the SiO−PVdF and SiO−PAA composite electrodes prepared with different amount of the binders are summarized in Figure 7. For the PVdF composite, intensity of each spectrum was not affected by the amount of the binder (silicon $2p_{3/2}$ spectra are shown in Figure 7a as one example).

Table 2. Summary of X-ray Photoelectron Spectroscopy for the SiO Composite Electrodes Prepared with 10 wt % PVdF and PAA Binders[a]

	atomic ratio (normalized with carbon)			
binder	carbon	silicon	oxygen	fluorine
PVdF	1	1.33	2.25	3.29
PAA	1	0.95	2.61	

[a] Atomic ratio is calculated from XPS spectra based on photoelectron intensity and their atomic sensitivity factors (normalized by the C 1s spectra).

This indicates that the SiO−PVdF composite exists as the mixture of SiO particles and PVdF crystalline bundles, therefore, bare SiO particles are still observed at the surface of the SiO−PVdF composite electrode prepared with 30 wt % of PVdF by XPS without the reduction of intensity from the SiO component.[25]

In contrast to the PVdF composites, peak intensity of Si $2p_{3/2}$ in the XPS spectra for the PAA composites is significantly influenced by the amount of the binders. Si $2p_{3/2}$ spectra are consisting of two components: elemental Si at 99.5−100 e V and SiO_2 at 103−104 eV. Both peaks can be assigned to the components of the SiO, which is segregated into Si and SiO_2 in its individual particles.[9] The intensity from both components is drastically weakened as the PAA content increases. Oxygen and carbon 1s spectra are shown in Figure 7c,d, respectively. The oxygen 1s spectra reflect the existence of both PAA and SiO_2. Carbon 1s spectra are mainly consisting of the components of the PAA polymer, not of acetylene black. The fraction of $-CH_2-$ and −COOH components increases as PAA content increases (Figure 7d), whereas SiO_2 component for oxygen 1s spectra decreases (Figure 7c). Table 2 compares atomic ratio of carbon,

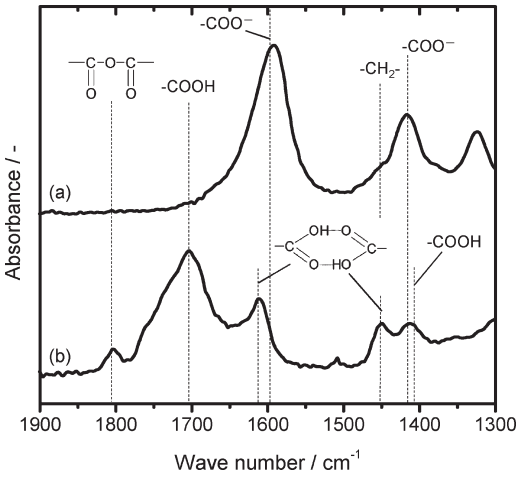

Figure 8. ATR-FTIR spectra of the cast films of (a) CMCNa and (b) PAA dried at 150 °C for 24 h in vacuum.

silicon, oxygen, and fluorine for 10% PAA and PVdF electrodes estimated from the XPS spectra. Clearly, a larger ratio of silicon at the electrode surface was observed for PVdF. These facts indicate that the polyacrylate became the dominant component at the surface of the SiO−PAA composite electrode. From these results, it is clear that the thin coating of the PAA binder effectively covers SiO particles and acetylene black in comparison to the PVdF, which is one of the reasons to show the strong adhesion ability.

Comparing the chemical character between PVdF and PAA, it is a general assumption that the carboxylic groups of the PAA binder play an important role in better uniformity and strong binding ability in the composite electrode due to its amorphous and cross-linking nature by hydrogen bond between carboxylic groups, but some questions still remain unclear. As shown in Figure 1, CMCNa and PAA polymers resemble each other in −COOH/−COONa functional groups, which could chemically interact with Si−OH group on the surface of SiO particles that should be formed in atmosphere as described previously.[12] Moreover, both polymers have similar characters as the amorphous polymer from XRD (Figure 6). However, the better cycle ability for the SiO−PAA composite electrode was obtained compared with the SiO−CMCNa. Hence, the difference in the interaction between polymers within the composite electrodes is further examined by ATR-FTIR spectroscopy.

Figure 8 compares ATR-FTIR spectra of the cast films of CMCNa and PAA on copper foil dried at 150 °C. The results confirmed similar characteristic features originating from the functional groups for both polymers. The main absorbance bands are assigned into the free carboxylic acid group (−COOH) at 1710 and 1410 cm^{-1} for the PAA, and the clear peaks of sodium carboxylate group ($-COO^{-}Na^{+}$) at 1600 and 1420 cm^{-1} with $-CH_2$ group at 1450 cm^{-1} for the CMCNa. Note that absorbance from the associated two carboxylic groups, forming hydrogen bonding to cross-link the PAA chain, can be found in the PAA film. In addition, an absorbance band is observed at 1800 cm^{-1}, which can be assigned into >C═O symmetrical stretching, indicating the formation of the carboxylic anhydride group. One possible explanation is that dehydration reaction of the associated carboxylic groups partially occurs by the drying process at 150 °C, resulting in the formation of carboxylic anhydride group (Supporting Information Figure S1). This is

Table 3. The Swelling Property of the Polymer Films in 1 mol dm^{-3} $LiPF_6$ EC/DMC

polymer films	weight gain after soaking in electrolyte solution/%
PVdF	43
CMCNa	13
PAA	8

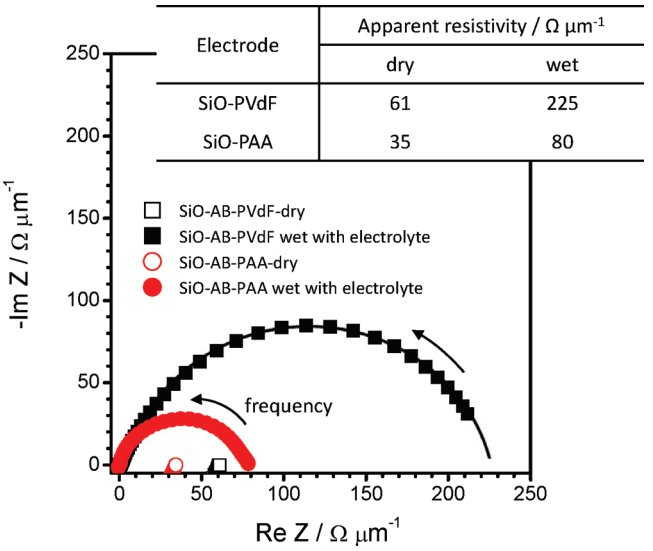

Figure 9. Through-thickness resistance of the SiO electrodes prepared with PVdF and PAA binder measured by impedance spectroscopy. Resistance of the electrodes was compared between before and after the soaking with electrolyte.

also supported by thermogravimetric measurement that confirmed the gradual weight loss of 10−20 wt % of pristine PAA powder by heating from room temperature to 150 °C in air (Supporting Information Figure S1). These facts imply that the linear polymeric chains of PAA are partly bridged and cross-linked by the hydrogen bonding and the carboxylic anhydride group forming the network polymer in the SiO composite. This change from the linear polymer to the polymeric cross-linkage network would modulate the mechanical/chemical properties against the large volume expansion in the composite electrode.

Furthermore, swelling property of the polymer films were examined by soaking them in the electrolyte solution at room temperature. Weight gain of the polymer films after the electrolyte soaking for 24 h is summarized in Table 3. The weight gain of PVdF polymer film by the absorption of the carbonate solution is much more evident compared to that of CMCNa and PAA. Weight gain of the PVdF reaches more than 40% of the initial weight of PVdF in this experimental condition, whereas the PAA film was less than 10% gain. These results indicate that the polymer composite easily swells when it is wet with the electrolyte. Supporting Information Figure S2 shows the photograph of the polymer powders before and after soaking in the electrolyte. When the electrolyte was added to the PVdF polymer powder, it was immediately wet with the electrolyte. A gel-like product was formed for PVdF after 1 day. In contrast to PVdF, apparent change in the PAA polymer powder was not observed visually. This is consistent results with the swelling test using the polymer films in Table 3.

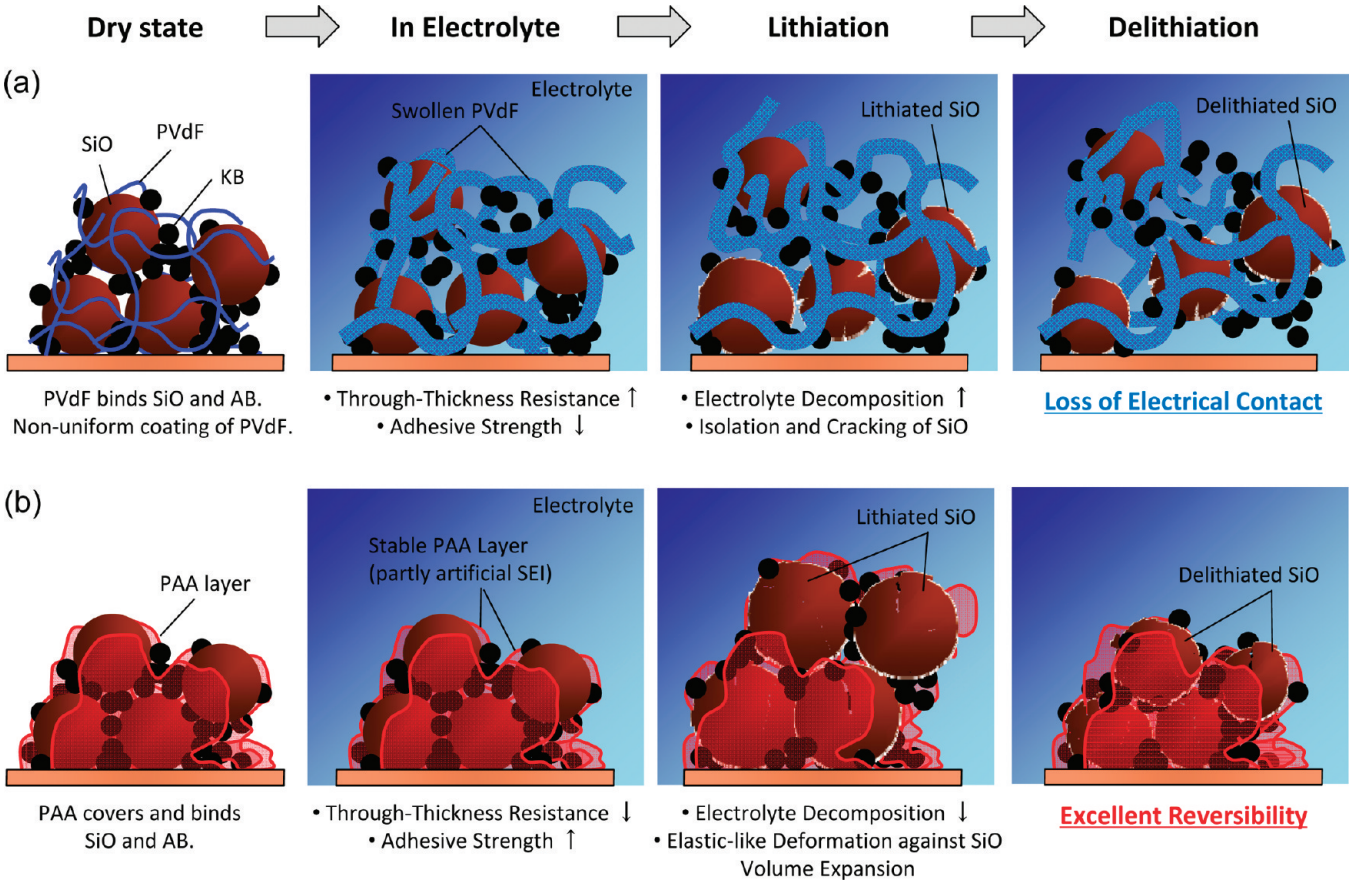

Figure 10. Schematic illustrations of the proposed mechanism for the improved cycleability for the SiO powder composite electrodes; (a) PVdF and (b) PAA binders. (See the text in detail.)

Such swelling character of the polymer films significantly influences the electronic conduction in the composite electrode as shown in Figure 9. Through-thickness apparent resistivity of the disk-type composite electrodes (thickness: 12 and 8 μm for PVdF and PAA, respectively) were measured by ac impedance method. The electrodes in dry state behave like a resistor as almost pure electric (electron) conductor. The through-thickness resistance of the composite electrodes is calculated to be 61 and 35 $\Omega\ \mu m^{-1}$ for PVdF and PAA electrodes, respectively. When the electrode is wetted by the electrolyte solution, the composite electrodes behave like a mixed conductor (both electron and ions), causing the frequency dependency of impedance as clearly seen in the Nyquist plots of Figure 9. Thus, the resistance is reduced at the higher frequency range compared to those in dry state because of the high ionic conductivity of the electrolyte solution absorbed in the electrode pores and binders. However, Figure 9 also confirms that the existence of the electrolyte solution in the composite electrode also deteriorates the electric conduction throughout the composite electrode, that is, the increase in the resistance of the composite electrodes, in the middle to the lower frequency range. As shown in Table 3 and Supporting Information Figure S2, PVdF easily swells by absorbing electrolyte, leading to the penetration of electrolyte solution into the whole composite electrode. The electrical conductive network in the PVdF composite electrode consisting of the active materials and conductive carbons might be in part loosen and/or broken by the penetration, therefore, the overall resistance of the PVdF composite electrode is significantly increased, compared to that of the PAA. Indeed, the through-thickness resistance of PVdF electrode is 3.5 times larger than that of the dry state. Although the resistance of the PAA composite electrode is also increased (approximately two times), the through-thickness resistance (80 $\Omega\ \mu m^{-1}$) is much smaller than that of the PVdF (225 $\Omega\ \mu m^{-1}$).

Improvement Mechanism for SiO−PAA Electrode. In this paper, we have shown that electrochemical properties were highly influenced by the selection of the binders and also preparation condition of the composite electrodes. From the XRD shown in Figure 6, the PVdF and PVA binders, which show poor electrochemical reversibility (Figures 2−4) as the binder for SiO, have both crystalline and amorphous regions. In general, strength, ductility, and toughness of the polymers depend on the fraction of the crystallite and amorphous regions. Crystalline polymers in dry condition show higher strength and less ductility in comparison to the amorphous polymer. On the other hand, the CMCNa and PAA binders, achieving better electrochemical activity of SiO, are the polymer consisting of mainly amorphous region (Figure 6). The difference of these two polymers was further revealed by the infrared spectroscopy (Figure 8). The carboxylic groups in the PAA polymer molecules are partly associated by the hydrogen bonding, which is partially transformed into the carboxylic anhydride group after the drying process. The hydrogen bonding and/or carboxylic anhydride group bind tightly polymer chains in the composite electrode, in other words, the chemically cross-linked network structures. Furthermore, the amorphous PAA in the SiO electrode may

dx.doi.org/10.1021/jp201691g |J. Phys. Chem. C 2011, 115, 13487–13495

Table 4. Self-Discharge Tests of PAA−SiO and PVdF−SiO (10 wt % binder) Composite Electrodes[a]

binder	capacity retention
PVdF	60%
PAA	95%

[a] Capacity retention rates in 5th cycle were compared after 10 days storage at room temperature after fully charging to 0.00 V.

have physical cross-linked structures, for example, loop and entanglement of the main chains. PVdF has no reactive group for the chemical cross-linking structures. In crystallized region of PVdF, the polymer main chains are tightly packed into the crystal domain, creating long-range ordering and/or bundle structure. This further reduces the fraction of the polymer used for the physical cross-linked structures.

From these considerations, the mechanism of the improved performance for the SiO−PAA composite electrode in comparison to the PVdF is summarized as follows, and schematics are shown in Figure 10. Since the PVdF composite electrode easily swells by absorbing electrolyte solution, the through-thickness resistance of the electrode increases when the electrolyte is added as already discussed in Figure 9. Interface area between the electroactive materials and electrolyte solution is also significantly increased. Thus the significant electrolyte decomposition must be inevitable during the lithiation process, simultaneously, the volume of SiO particles increases up to 200% of the initial volume. For both PVdF and PAA binders, it would result in fracture of the SiO particles. PVdF, which is high crystallinity polymer, has less cross-linked structures and less coverage on SiO particles compared with the amorphous PAA polymer, and no chemical interaction between PVdF molecules and SiO exists because of chemical inactivity of PVdF so that the adhesive peel strength of the PVdF composite is not strong (Table 1). We confirmed by handling that the strength is further weakened when it is wet with the electrolyte. By the stress induced by volume expansion of the lithiation SiO, the conduction network of the SiO−PVdF on current collector is readily deformed. During the delithiation process, the volume of the fractured SiO particles is contracted, subsequently, a large part of SiO particles is electronically isolated in the composite electrode.

On the other hand, the PAA polymer uniformly covers the SiO particles because the amorphous character of PAA polymer would maximize the physical cross-linked structures in the uniform PAA film covering SiO particles as mentioned in Figures 7 and 8. Moreover, the interaction between its carboxylate groups and the hydroxide groups on SiO surface formed by exposure to atmosphere probably helps the uniform coverage. The carboxylic anhydride group chemically cross-links the polymer chains that enhance the mechanical strength. As a result, adhesive strength of the PAA composite electrode to the cupper current collector is much better than that of the PVdF composite electrode (Table 1). As shown in Table 3 and Supporting Information, Figure S2, the PAA polymer layers can suppress the swelling of the SiO composite compared to the PVdF. The through-thickness resistance of the electrode is much lower than that of the PVdF composite even after the addition of the electrolyte (Figure 9). Thus, the uniform polymer coating reduces the net contact area between electrolyte and electroactive materials. In other words, the polyacrylate coating layer partly acts as an artificial SEI layer on the negative electrodes in lithium-ion cell,[19−21,24] resulting in the suppression of irreversible decomposition at the SiO electrode. To test this hypothesis, a self-discharge test of SiO−PAA composite in lithium cell has been conducted and compared to that of SiO−PVdF composite electrode as shown in Table 4. If the uniform SEI layer exists on the SiO particles, the self-discharge will be suppressed on the basis of passive SEI proposed by Peled.[26] When the electrochemical cells were cycled in the voltage range of 2.0−0.0 V at a rate of 100 mA g^{-1} in Figure 4, the cells were allowed to rest for 5 min after each charge/discharge step. To examine self-discharge, the cells rested for 10 days at room temperature only after the fifth charge step. Coulombic efficiency of the PAA composite in the fifth cycle reaches 95% in this experimental condition. In contrast to the PAA binder, a self-discharge rate of the SiO−PVdF composite electrode significantly accelerates. Coulombic efficiency of the PVdF composite is approximately 60% in the same condition with the PAA composite. The results strongly support our hypothesis described above. The PAA layer behaves in the similar way to that of SEI.

However, an important question still remains unclear. How does the PAA binder act on the huge volume expansion of SiO particles during the lithiation? It is speculated that these physical and chemical cross-linked structures in the PAA polymer layer allow elastic-like deformation without breaking of the polymer networks, against the mechanical stress induced by large volume expansion of the lithiated SiO particles. The fracture of each SiO particle cannot be suppressed by the binder, however, the PAA thin layer on SiO can hold fractured SiO particles and suppress the collapse of the electrode morphology resulting in the maintenance of the electronical conduction throughout the electrode during cycling; thereby the cycleability of the SiO−PAA polymer is highly improved.

For the practical lithium-ion batteries, active electrode materials are powders of graphite, $Li_{4/3}Ti_{5/3}O_4$, $LiCoO_2$, Li(Ni,Mn,Co)O_2, $LiMn_2O_4$, and so on. In order to apply the powdery electrode materials, we should make the composite electrode by mixing with conductive additive and binder as is used generally. Because the conductive additive and binder are electrochemically inactive, their amount has to be reduced to maximize both energy/power density of the batteries, for example, Ketjen black and (styrene-butadiene rubber)-CMCNa can be used instead of acetylene black and PVdF, respectively. In this study, we clarify that chemical and physical nature of polymeric binder is also important to design the state-of-the-art lithium ion battery, such as alloying and conversion with lithium. The complex effectiveness of functional binders depending on molecular structure including cross-link, slurry, binding condition, adhesion state onto current collector, crystallinity, interfacial morphology, swelling with electrolyte, and so forth will realize the improvement of electrode performance for the batteries. The binder chemistry for lithium ion batteries has high potential to enhance the battery performance and to control interface structure including SEI.

CONCLUSIONS

We examined the high-capacity SiO−powder composite electrodes prepared with different polymer binders, which were characterized by ATR-FTIR, XRD, XPS, peel tester, and electrochemical method. The electrochemical activity of the SiO composite electrode is significantly improved by using the PAA binder in comparison to the conventional PVdF binder. The

SiO−PAA composite electrode can deliver more than 700 mAh g^{-1} of rechargeable capacity with excellent cycleability at a rate of 100 mA g^{-1}. It was found that the PAA polymer is mainly amorphous form confirmed by XRD, whereas the PVdF binder has the crystallized region. The amorphous region increases the physical/chemical cross-linked structures in the SiO−PAA composite electrode. XPS study suggested that the SiO particles are uniformly covered by the PAA polymer in comparison to the PVdF binder. SEM observation clearly demonstrated that the collapse of the SiO powder based composite electrode was effectively suppressed by the thin coating layer of the PAA binder. In this paper, we have clearly demonstrated that the polymer binder has the huge impact on the electrochemical activity of the powder based composite electrodes. We believe that such methodology will have certain advantage for the development of the lithium-ion battery technology in the future.

■ ASSOCIATED CONTENT

Supporting Information. Additional information. This material is available free of charge via the Internet at http://pubs.acs.org.

■ AUTHOR INFORMATION

Corresponding Author
*E-mail address: komaba@rs.kagu.tus.ac.jp.

■ ACKNOWLEDGMENT

This work was financially supported by KAKENHI (No. 21750194), NEDO, and the Funding Program for Next Generation World-Leading Researchers, JSPS, Japan.

■ REFERENCES

(1) Obrovac, M. N.; Christensen, L. *Electrochem. Solid State Lett.* **2004**, *7*, A93.
(2) Komaba, S.; Mikami, F.; Itabashi, T.; Baba, M.; Ueno, T.; Kumagai, N. *Bull. Chem. Soc. Jpn.* **2006**, *79*, 154.
(3) Li, H.; Huang, X. J.; Chen, L. Q.; Wu, Z. G.; Liang, Y. *Electrochem. Solid State Lett.* **1999**, *2*, 547.
(4) Maranchi, J. P.; Hepp, A. F.; Kumta, P. N. *Electrochem. Solid State Lett.* **2003**, *6*, A198.
(5) Moon, T.; Kim, C.; Park, B. *J. Power Sources* **2006**, *155*, 391.
(6) Buqa, H.; Holzapfel, M.; Krumeich, F.; Veit, C.; Novak, P. *J. Power Sources* **2006**, *161*, 617.
(7) Beattie, S. D.; Larcher, D.; Morcrette, M.; Simon, B.; Tarascon, J. M. *J. Electrochem. Soc.* **2008**, *155*, A158.
(8) Morimoto, H.; Tatsumisago, M.; Minami, T. *Electrochem. Solid State Lett.* **2001**, *4*, A16.
(9) Kim, T.; Park, S.; Oh, S. M. *J. Electrochem. Soc.* **2007**, *154*, A1112.
(10) Yang, J.; Takeda, Y.; Imanishi, N.; Capiglia, C.; Xie, J. Y.; Yamamoto, O. *Solid State Ion.* **2002**, *152*, 125.
(11) Ohzuku, T.; Iwakoshi, Y.; Sawai, K. *J. Electrochem. Soc.* **1993**, *140*, 2490.
(12) Hochgatterer, N. S.; Schweiger, M. R.; Koller, S.; Raimann, P. R.; Wohrle, T.; Wurm, C.; Winter, M. *Electrochem. Solid State Lett.* **2008**, *11*, A76.
(13) Chen, L. B.; Xie, X. H.; Xie, J. Y.; Wang, K.; Yang, J. *J. Appl. Electrochem.* **2006**, *36*, 1099.
(14) Li, J.; Lewis, R. B.; Dahn, J. R. *Electrochem. Solid State Lett.* **2007**, *10*, A17.
(15) Lestrie, B.; Bahri, S.; Sandu, I.; Roue, L.; Guyomard, D. *Electrochem. Commun.* **2007**, *9*, 2801.
(16) Ding, N.; Xu, J.; Yao, Y. X.; Wegner, G.; Lieberwirth, I.; Chen, C. H. *J. Power Sources* **2009**, *192*, 644.
(17) Bridel, J. S.; Azais, T.; Morcrette, M.; Tarascon, J. M.; Larcher, D. *Chem. Mater.* **2010**, *22*, 1229.
(18) Ozeki, T.; Shimomura, K.; Komaba, S.; Yui, H.; Katayama, Y.; Miura, T. In The 76th Annual Meeting of the Electrochemical Society of Japan, Kyoto, Japan, March, 2009; Electrochemical Society of Japan: Tokyo, 2009; pp 357.
(19) Komaba, S.; Okushi, K.; Ozeki, T.; Yui, H.; Katayama, Y.; Miura, T.; Saito, T.; Groult, H. *Electrochem. Solid State Lett.* **2009**, *12*, A107.
(20) Komaba, S.; Ozeki, T.; Okushi, K. *J. Power Sources* **2009**, *189*, 197.
(21) Komaba, S.; Ozeki, T.; Yabuuchi, N.; Shimomura, S. *Electrochemistry* **2011**, *79*, 6.
(22) Magasinski, A.; Zdyrko, B.; Kovalenko, I.; Hertzberg, B.; Burtovyy, R.; Huebner, C. F.; Fuller, T. F.; Luzinov, I.; Yushin, G. *ACS Appl. Mater. Interfaces* **2010**, *2*, 3004.
(23) Miyachi, M.; Yamamoto, H.; Kawai, H.; Ohta, T.; Shirakata, M. *J. Electrochem. Soc.* **2005**, *152*, A2089.
(24) Komaba, S.; Yabuuchi, N.; Ozeki, T.; Okushi, K.; Yui, H.; Konno, K.; Katayama, Y.; Miura, T. *J. Power Sources* **2010**, *195*, 6069.
(25) Hirasawa, K. A.; Nishioka, K.; Sato, T.; Yamaguchi, S.; Mori, S. *J. Power Sources* **1997**, *69*, 97.
(26) Peled, E. *J. Electrochem. Soc.* **1979**, *126*, 2047.